Analyst

PAPER

View Article Online
View Journal | View Issue

Cite this: *Analyst*, 2016, **141**, 5144

Unforeseen distance-dependent SERS spectroelectrochemistry from surface-tethered Nile Blue: the role of molecular orientation†

Andrew J. Wilson and Katherine A. Willets*

Received 2nd June 2016,
Accepted 20th June 2016

DOI: 10.1039/c6an01266c

www.rsc.org/analyst

Covalent immobilization of redox-active dyes is an important strategy to evaluate structure–activity relationships in nanoscale electrochemistry by using optical readouts such as surface-enhanced Raman scattering (SERS). Here we investigate the role of the tether length in the SERS spectroelectrochemistry of surface-attached Nile Blue. Differential pulse voltammetry and a potential-dependent SERS derivative analysis reveal that the Nile Blue molecules adopt a different orientation with respect to the electrode surface as the number of carbons in a carboxylic acid-terminated alkanethiol monolayer is varied, which leads to unique SERS spectroelectrochemical behaviors. We use the relative molecular orientations and spectral characteristics to propose a model in which tethers shorter than the length of the molecule limit molecular motion under electrochemical perturbation, but tethers longer than the length of the molecule allow dye intercalation into the hydrophobic self-assembled monolayer, producing an unexpected decrease in the SERS intensity when the molecule is in the oxidized form.

Introduction

Surface-enhanced Raman scattering (SERS) is a powerful tool for studying the electrochemical performance of redox reactions on nanoscale electrodes due to its single molecule sensitivity, chemical specificity, and sensitivity to local environmental changes.[1–3] The redox dye Nile Blue (NB) has emerged as an excellent probe for probing fundamental electrochemistry with SERS.[4–10] A key feature of NB is that resonant excitation (*e.g.* 642 nm) leads to a strong SERS signal when the molecule is in its oxidized form and a weak SERS signal when it is in its reduced form, providing a spectral readout for reduction and oxidation events (*e.g.* Fig. 1A). In addition to its redox-dependent spectral signatures, which are detectable down to the single molecule level,[4] NB is attractive because it can be immobilized on noble metal electrodes, allowing the possibility of structure–activity correlation.[8,11] Molecules tethered to an electrode, however, will have electrochemical behaviors different from their solvated analogues, where diffusion or convection control the current response. Furthermore, the nature of the tether (*e.g.* length, organization) can alter interfacial interactions, such as electrode–molecule separation and molecular orientation, which have been shown to vary the electrochemical response.[6,12] Therefore, to appropriately apply SERS spectroelectrochemistry to nanoelectrochemical phenomena, investigation of the impact of the tether is necessary.

Fig. 1 highlights a previous example from our group in which tethering the NB molecules to a nanoelectrode altered the SERS spectroelectrochemical response.[8] Fig. 1A shows the

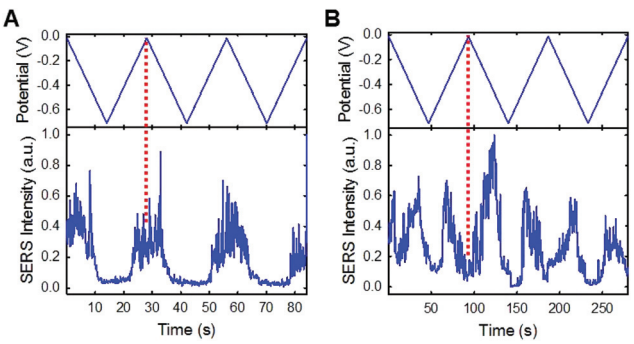

Fig. 1 Electrochemically-modulated integrated SERS intensity from diffraction-limited noble metal colloidal aggregates labeled with Nile Blue. (A) SERS from NB physisorbed on Ag nanoparticles modulated at a scan rate of 50 mV s^{-1}. (B) SERS from NB covalently immobilized on Au nanoparticles modulated at a scan rate of 15 mV s^{-1}. Red dashed lines indicate the SERS intensity at the positive switching potential and highlight the intensity difference between the physisorbed and tethered form of NB. Adapted with permission from ref. 8. Copyright 2015 American Chemical Society.

Department of Chemistry, Temple University, Philadelphia, PA 19122, USA.
E-mail: kwillets@temple.edu

†Electronic supplementary information (ESI) available: Electrode stabilization, divot depth, spectral fits. See DOI: 10.1039/c6an01266c

integrated SERS intensity from NB physisorbed onto Ag colloidal aggregates as a function of applied potential. Consistent with previous reports,[4,7,9,10] as the potential is swept positive (negative) of the formal potential of the NB redox reaction ($E^{\circ} \approx -0.25$ V), the SERS intensity gradually increases (decreases) to a constant average value, indicating complete oxidation (reduction) of all NB molecules on the surface. However, in subsequent work from our lab, we immobilized the NB on spherical Au nanoparticle aggregates *via* carbodiimide coupling to a carboxylic acid-terminated alkanethiol self-assembled monolayer (SAM) to prevent molecule diffusion and desorption.[8] In contrast to the physisorption case, Fig. 1B shows that in the anodic scan, the SERS intensity initially rises, as expected, then falls to a minimum intensity value at the most positive potential (red dashed lines in Fig. 1). Sweeping back towards negative potentials, the SERS intensity initially rises before falling to the minimum intensity value, as expected, when all NB molecules are reduced. The reproducible drop, or divot, in the SERS intensity at the most oxidizing potentials persists over many potential cycles, and is observed over a large range of nanoparticle structures and plasmonic substrates that were investigated, suggesting that the tether is responsible for the emergence of this unexpected spectral behavior.

To understand the anomalous SERS spectroelectrochemical behavior of the tethered Nile Blue, we recently compared the electrochemistry of both physisorbed and covalently-tethered NB on plasmonic gold electrodes.[13] Several reports of NB physisorbed on plasmonic substrates have shown electrochemical behaviors that follow solution phase NB: a single peak in the cyclic voltammogram (CV) that corresponds to a two electron transfer process accompanied by either one or two protons depending on the pH of the buffered electrolyte.[4,9,14] Our group found that tethering NB to Au electrodes *via* carbodiimide chemistry changes its electrochemical properties such that two individual peaks emerge in the differential pulse voltammogram (DPV), each corresponding to a one electron, one proton redox reaction (Fig. 2).[13] We identified the low and high energy peaks in the DPV as the electrochemical (de)protonation of the terminal amine and the phenoxazine nitrogen in the tethered NB, respectively. This emergent electrochemical behavior is unique to NB tethered *via* carbodiimide linking chemistry and is not observed when the NB is tethered using azide–alkyne "click" chemistry. As anticipated, the new electrochemical features also led to SERS intensity changes associated with each of these redox reactions, allowing us to assign the specific protonation sites associated with each electron transfer event.

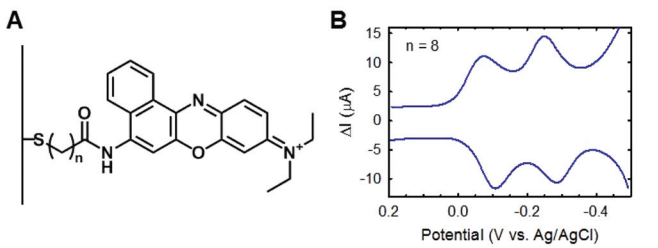

Fig. 2 (A) Structure of NB tethered to a carboxylic-acid terminated self-assembled monolayer *via* carbodiimide linking chemistry. (B) Differential pulse voltammogram of surface-tethered NB shows the emergence of two distinct redox peaks, in contrast to solution-phase or physisorbed NB which show only a single redox peak. Adapted with permission from ref. 13. Copyright 2016 American Chemical Society.

In the current study, we probe the distance-dependent SERS spectroelectrochemistry of NB covalently tethered to nanoscale roughened Au films known as island films (AuIFs).[15] Electrode–molecule distance is known to alter both the SERS intensity and the electrochemical response of probe molecules,[16–19] and because physisorbed and covalently-attached molecules have different distances to the electrode, we hypothesized that the electrode–molecule distance could produce the different potential-dependent SERS behaviors shown in Fig. 1. AuIFs are attractive substrates for these studies because in addition to providing plasmonic enhancement due to nanoscale features, they are also quasi-transparent, in direct electrical contact with the supporting substrate electrode, and (as prepared) do not have ligands on the electrode surface which can both impede electron transfer and alter the formation of self-assembled monolayers (SAMs). AuIFs can also be prepared over large areas, which enables an ensemble behavior of NB spectroelectrochemistry to be measured.

In our covalent attachment strategy, we control the electrode–molecule distance by changing the number of carbon atoms in the carboxylic acid-terminated alkanethiol molecule used as a molecular linker. However, it is important to note that short alkanethiol chains with carboxylic acid functional groups are known to contain defects in the SAM monolayer, although longer chains produce a more crystalline monolayer.[20] Additionally, our nanoscale rough electrodes will inherently introduce monolayer defects at the ensemble level. Therefore, we aim to qualitatively assess the impact of changing the number of carbons in the alkanethiol chain on the spectroelectrochemical response of tethered NB, while acknowledging that some surface defects are to be expected due to the nature of the AuIF substrate and may lead to a range of molecular–electrode distances for a given tether length. Despite these challenges, we find trends in the distance-dependent SERS spectroelectrochemistry of the tethered NB that enable us to propose a mechanism for the SERS intensity divots based on changes in molecular orientation.

Experimental methods

Electrode preparation

Indium tin oxide (ITO) coated glass coverslips were cleaned by sequential sonication in acetone, isopropyl alcohol, and water (18.2 MΩ cm) for 15 min in each solvent. AuIFs were prepared on top of the ITO coverslips by thermally evaporating Au at a rate of 0.5 Å s^{-1} until a thickness of 7 nm was reached. The as-prepared Au electrodes were found to be high quality, as

revealed by stable voltammograms being achieved after only 3 redox cycles in sulfuric acid and stability maintained for more than 30 cycles.[13] Immediately following Au deposition, the AuIFs were incubated in a 10 mM ethanolic solution of a carboxylic acid-terminated alkanethiol for 48 hours to coat the Au with a SAM. Previous work using 8-mercaptooctanoic acid SAMs showed monolayer surface coverage under these conditions.[13] The carboxylic acid alkanethiol tether molecules were systematically varied as follows to alter the electrode–molecule distance: 3-mercaptopropionic acid (3MPA), 6-mercaptohexanoic acid (6MHA), 8-mercaptooctanoic acid (8MOA), 11-mercaptoundecanoic acid (11MUA), and 16-mercaptohexadecanoic acid (16MHDA).

1-Ethyl-3-(3-dimethylaminopropyl)carbodiimide hydrochloride (EDC) and *N*-hydroxysulfosuccinimide (NHS) were used to couple the primary amine of NB to the carboxylic acid groups of the SAM tether molecules. An aqueous mixture of 0.02 M EDC and 0.04 M NHS were incubated over the AuIF@SAM samples for 1 hour in a humid environment. After rinsing the excess reagents away, the activated AuIF@SAM samples were incubated in a solution of 10 μM NB in 0.1 M phosphate buffer at pH 5 for 4 hours. Acetone and water were used to wash the samples to remove as much physisorbed NB as possible.

With NB tethered to the AuIFs, an electrochemical cell was fabricated. First, a tinned-copper wire was fastened to the ITO with Ag conductive epoxy. The epoxy was cured at ~150 °C for 15 min. Meanwhile, four glass slides were cut and attached together with clear epoxy to form a hollow rectangle. Finally, the glass walls were attached to the ITO/AuIF surface with clear epoxy to form a well. For all experiments a Pt wire was used as a counter electrode, Ag/AgCl (1 M KCl) was employed as a reference electrode, and a 0.1 M phosphate buffer at pH 5 served as the electrolyte. Unless otherwise noted, CV measurements were performed at a scan rate of 10 mV s^{-1} and DPV measurements were made with pulses of 50 mV in amplitude, 50 ms in duration, and a 500 ms period using a 650E CH Instruments potentiostat. The potential was cycled across the NB redox window until a stable current was reached as determined with DPV for each electrode (Fig. S1 and S2†).

Spectroelectrochemical methods

Wide-field optical microscopy measurements were made using a 20× objective to focus a circularly polarized 642 nm laser beam to the sample plane of an Olympus IX-71 inverted microscope. The resulting emission was collected back through the same objective in an epi-illumination geometry. A 50/50 beamsplitter was placed in the microscope detection path for simultaneous collection of: (a) SERS spectra (1 s integration) using a Princeton Instruments Isoplane SCT320 spectrometer and a ProEM 1600 electron-multiplied CCD (EMCCD) and (b) SERS images (200 ms integration) with a Princeton Instruments ProEM 512 EMCCD. The electrochemical cells were mounted on the microscope stage, filled with buffer, and wired to the potentiostat. The applied potential program was initiated at the start of data acquisition for time synchronization between spectra, images, and potential.

Results and discussion

Fig. 3 shows the SERS spectroelectrochemical response of NB as the tether length is increased by changing the number of carbons in the linker from 3 to 16. The left column of Fig. 3 shows a series of SERS cyclic voltammograms (SERS-CVs) following the intensity of the 588 cm^{-1} mode of NB as a function of both applied potential and linker length. The 588 cm^{-1} mode reports on the CNC deformation of the phenoxazine moiety in NB,[9,21] allowing it to serve as a diagnostic peak for changes associated with the phenoxazine ring.[13] For all tether lengths explored, the 588 cm^{-1} SERS intensity is at a minimum at the most negative potentials and then slowly rises as the potential is swept across the phenoxazine formal potential (−0.4 V to −0.2 V). Upon reaching oxidizing potentials (*i.e.* −0.2 V to +0.2 V) for phenoxazine, the NB attached *via* the shortest linker containing 3 carbons (Fig. 3A) shows a relatively stable SERS intensity, consistent with the behavior of physisorbed NB (Fig. 1A). However, as the length of the linker doubles to 6 carbons (Fig. 3B), a small drop in the 588 cm^{-1} SERS intensity is observed at oxidizing overpotentials. A more pronounced change in the SERS intensity occurs when the tether length is increased to 8 carbons (Fig. 3C) where a significant spectral intensity divot is observed at oxidizing overpotentials. Interestingly, at this transition the SAM tether is approximately the same length as the NB molecule. The depth of the spectral intensity divot continues to increase with an 11 carbon tether (Fig. 3D) and appears to saturate with a 16 carbon tether (Fig. 3E and S3†).

Next, we examine how the total SERS intensity changes as a function of both applied potential and linker length. For these studies, we take wide-field images of the illuminated region of interest and integrate the total SERS intensity over the image as a function of applied potential (Fig. 3, center column). Unlike the 588 cm^{-1} mode, which reports primarily on changes associated with the phenoxazine ring,[9,21] the total SERS intensity should reflect all emission sources (including weak background fluorescence from the molecule) and thus reveal the behavior of the NB across the full spectral window. For each tether length, two inflection points are seen in the integrated intensity SERS-CVs (Fig. 3, middle column), one for each redox reaction observed in the DPV (Fig. 2B). To visualize this more clearly, we take first derivatives of each of the integrated SERS-CVs and normalize them to their maximum value (Fig. 3, right column). The inflection points in the original SERS-CVs show up as peaks in the derivative plots, and the potentials associated with these peaks not only match extremely well with the peak potentials of the DPVs but are also independent of linker length.

We next examine the magnitude of the slopes associated with the rise/fall of the SERS intensity, which we expect to be

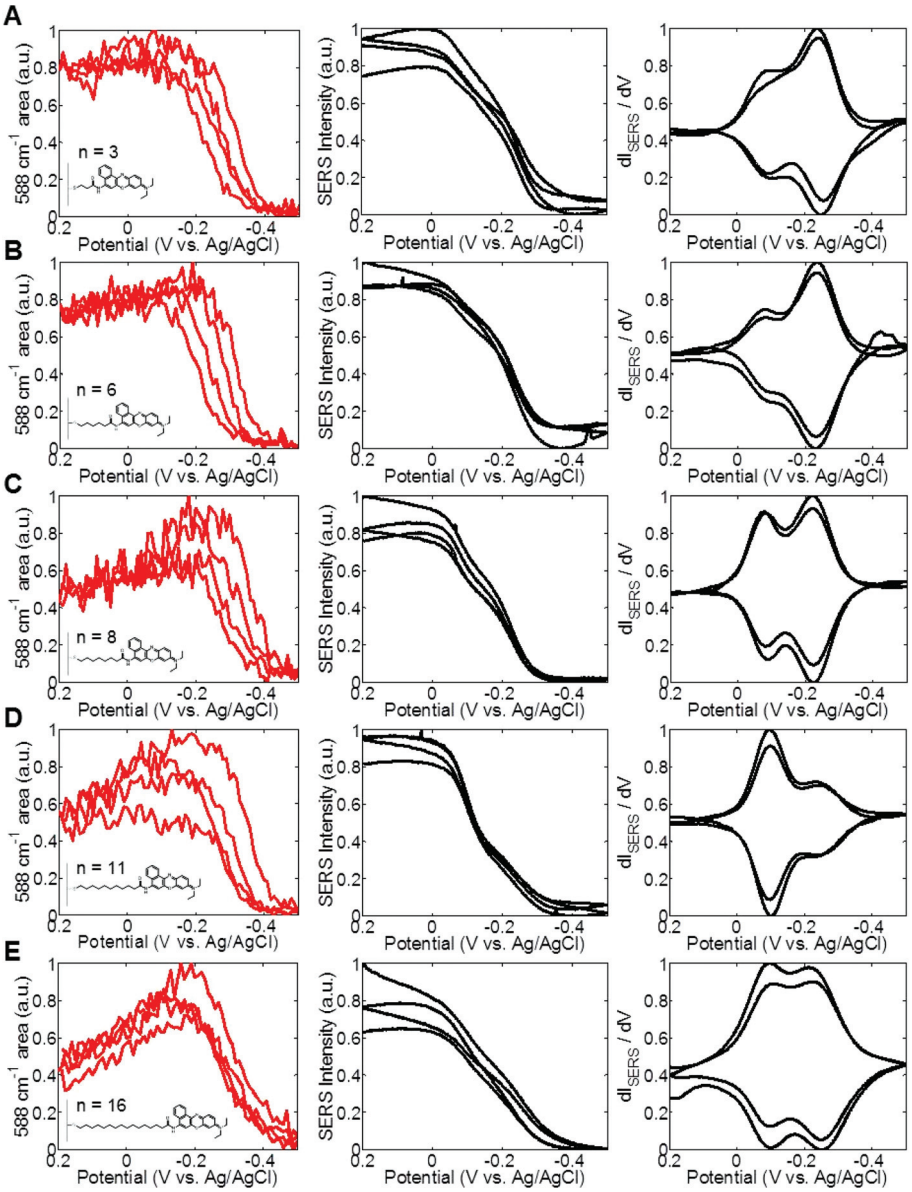

Fig. 3 NB SERS electrochemistry as a function of different tether lengths: (A) 3MPA, (B) 6MHA, (C) 8MOA, (D) 11MUA, (E) 16MHDA. (Left column) Integrated SERS intensity of the 588 cm^{-1} mode of NB as a function of applied potential. (Middle column) Integrated SERS intensity over all energies as a function of applied potential. (Right column) First derivative of the integrated SERS intensity with respect to potential.

proportional to the rate of electron transfer between the electrode and molecule. In the normalized first derivative plots, the heights of the two peaks observed for the reduction and oxidation processes (down and up peaks, respectively) represent the fastest electron transfer rate. As the tether length increases from 3 to 11 carbons, the magnitude of the peak height associated with the amine (de)protonation (occurring at more positive potentials) increases relative to the magnitude of the peak height associated with the phenoxazine (de)protonation (occurring at more negative potentials). Due to the well-known phenomenon of distance-dependent electron transfer, it is probable that the increase in the rate of electron transfer associated with the amine peak relative to the phenoxazine peak indicates that the amine moiety is moving closer to the electrode surface compared to the phenoxazine moiety as the linker increases from 3 to 11 carbons.[18,19] A limit is observed with a 16 carbon tether, however. In this case, the normalized heights of the two peaks are approximately equal between the amine and phenoxazine parts.

While the normalized derivative plots show a qualitative transition in relative electron transfer rates (*i.e.* SERS slopes) between the amine and phenoxazine reactions as the tether length changes, we can directly compare the rates by tabulating the magnitude of the peaks in the SERS derivative plots before normalization, then normalizing these values against the maximum slope associated with the oxidation of NB

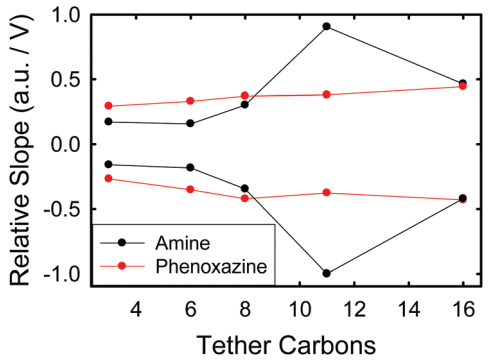

Fig. 4 Peak slopes for the amine (black) and phenoxazine (red) redox reactions of Nile Blue tabulated from the SERS image derivative plots. Each slope was normalized to the reduction of the amine peak at 11 carbons. Positive values represent oxidation rates and negative values represent reduction rates.

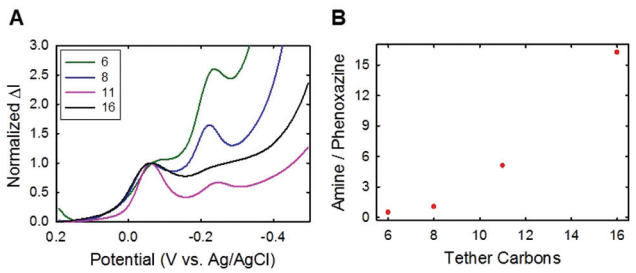

Fig. 5 (A) Cathodic differential pulse voltammograms of NB EDC coupled to 6MHA (green), 8MOA (blue), 11MUA (magenta), and 16MHDA (black) normalized to the amine redox reaction peak. (B) Charge ratio of the amine to phenoxazine redox reactions obtained by integration of the peaks in (A).

attached *via* the 11 carbon tether. Fig. 4 shows how the relative slopes of the SERS-CVs change for the two redox reactions as the length of the tether is increased. For a given linker length and redox reaction (*e.g.* amine or phenoxazine), the relative slopes are approximately equal in magnitude for both oxidation (negative slopes) and reduction (positive slopes) events, indicating good reversibility of the reaction. As the number of carbons in the tether increases from 3 to 11, the slope, and therefore relative electron transfer rate, of the amine reaction increases, which suggests that the amine is getting closer to the electrode surface despite the longer linker length. However, this trend reverses for the 16 carbon linker, indicating that once some critical distance is reached, the electron transfer rate slows.

In addition to the SERS spectroelectrochemical data, we can also extract distance-dependent trends in the DPV data for NB attached to the AuIF electrodes *via* different linkers. Unfortunately, in these experiments, the labeling density of NB tethered to 3MPA was inconsistent and the currents were often below the limit of detection of DPV; thus these data were excluded from the electrochemical analysis. For each experiment, the DPVs initially show signatures of both tethered and untethered NB (Fig. S1 and S2†), based on the large phenoxazine peak (which overlaps with the solution-phase peak of NB) relative to the amine peak. However, after repeated potential cycles, the magnitude of the phenoxazine peak stabilizes, indicating successful expulsion of the untethered molecules; this point will be revisited later in this manuscript. Fig. 5A shows DPVs of NB tethered *via* different length linkers following electrochemical stabilization, in which the differential current is normalized to the peak associated with the amine reduction reaction ($E^{\circ} \approx -0.05$ V). These data show that the peak differential current of the amine peak increases relative to the phenoxazine peak as the linker length increases (note that hydrogen production and charging currents are higher for the shorter length SAMs, suggesting possible higher defect density in these films, consistent with expectations).[20] Fig. 5B plots the ratio of the charge produced by the two redox reactions as a function of the number of carbons in the tether and shows that far more charge is passed to the amine moiety than the phenoxazine moiety as the molecule–electrode distance increases.

Based on these data, we now propose a mechanism that explains both the intensity divots in the SERS spectroelectrochemical data (Fig. 3), as well as the distance-dependent changes in the relative electron transfer rate (Fig. 4) and amount of charge consumed between the amine and phenoxazine associated reactions (Fig. 5). For the linkers with lengths that exceed the size of the NB molecule (8, 11, and 16 carbons), the oxidized form of the NB is able to intercalate into the SAM layer on the surface, consistent with previous descriptions of NB as a lipophilic dye.[22,23] Given that the NB is tethered *via* its primary amine, the insertion of the oxidized NB into the SAM leads to the tertiary amine pointing down toward the electrode surface (Fig. 6A, blue). For the linkers that are shorter than the size of the NB molecule (3 and 6 carbons), the NB is unable to intercalate into the SAM, leading to the tertiary amine residing further from the electrode surface (Fig. 6B, blue). The result is that the tertiary amine group of the oxidized NB is unexpectedly closer to the electrode surface when it is tethered to the longer linker (*e.g.* $d_{1,\mathrm{long}} < d_{1,\mathrm{short}}$ in Fig. 6), resulting in faster electron transfer rates to the amine as the linker length increases, as shown in Fig. 4. However, in linker lengths with fully intercalated NB molecules (11 and 16 carbons), increasing the number of carbon atoms in the linker increases the distance between the electrode and amine moiety, and thus leads to a decrease in the electron transfer rate.

Similar to the ejection of untethered NB following the reduction of the tertiary amine group (Fig. S1 and S2†), a reduced molecule tethered by the longer linkers is no longer stabilized by the SAM layer and reorients into bulk solution, further from the electrode surface ($d_{2,\mathrm{long}}$, Fig. 6A, red). In other words, the lipophilicity of NB decreases upon electrochemical reduction causing the molecules to migrate out of the hydrophobic SAM. At this new distance, the second reduction step associated with the phenoxazine moiety

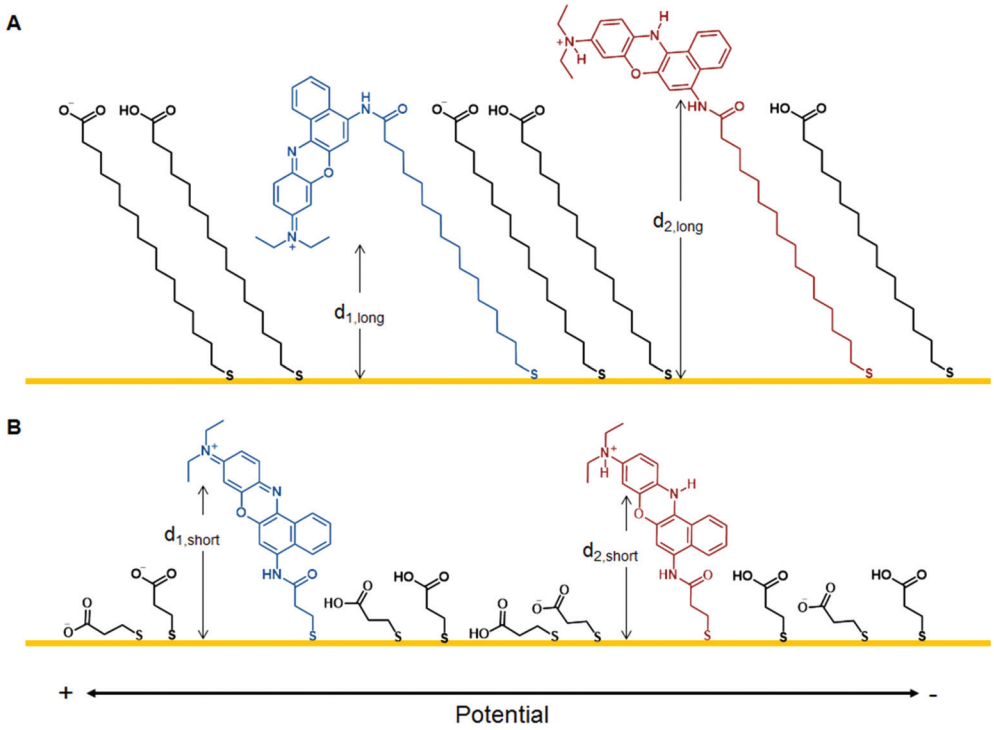

Fig. 6 Proposed schematic of the relative orientation of NB tethered to gold surfaces by (A) 16MHDA and (B) 3MPA. Blue molecules represent the fully oxidized form of NB and red molecules represent the fully reduced form.

becomes less favourable, resulting in less charge being transferred, consistent with the data in Fig. 5B. However, for the shorter chain tethers where the NB cannot intercalate into the SAM, the distance of the NB molecule from the surface does not significantly change ($d_{1,short} \approx d_{2,short}$) such that the ratio of charge transferred for the amine and phenoxazine moieties is roughly one, as observed (Fig. 5). This mechanism also explains why the relative peak heights in the SERS derivative plots in Fig. 3 (right column) change as a function of linker length: as the linker length increases, the amine peak (at more positive potentials) begins to dominate the phenoxazine peak (at more negative potentials) because the amine moiety is closer to the surface than the phenoxazine moiety (*e.g.* $d_{1,long} < d_{2,long}$) resulting in faster electron transfer.

While this mechanism is consistent with all of the electrochemical data we have presented, the distance-dependent loss in the 588 cm^{-1} SERS intensity at the most positive potentials (Fig. 3, left column) seems inconsistent with the mechanism. After all, we would expect that the closer the molecule is to the surface, the stronger the SERS signal would be, which is opposite of what we observe experimentally. However, the intercalation of the NB into the SAM results in a change in the orientation of the NB molecule, such that its transition dipole is oriented roughly vertical to the plane of the sample. In this conformation, our circularly polarized excitation traveling normal to the sample plane does not efficiently excite the NB, resulting in a loss of SERS intensity. The 588 cm^{-1} mode continues to decrease at potentials well positive of NB oxidation, which suggests that the electrode polarity is also influencing the orientation of the transition dipoles.[24] Moreover, when the solvatochromic NB intercalates into the hydrophobic SAM, we expect the absorption to shift to higher energies, resulting in a loss of resonance enhancement.[25–27] These effects most likely work in concert to generate a decrease in SERS intensity when the oxidized form of NB intercalates into the SAM on the electrode surface.

As further evidence for intercalation of the untethered NB, we calculate the charge consumed by the phenoxazine reaction near −0.2 V during the first reduction scan and compare it to the charge consumed during the 30th reduction scan. We find that while the charge only goes down by a factor of two for the 6-carbon linker, it decreases by a factor of 10 for the 11-carbon linker and a factor of 50 for the 16-carbon linker. This difference supports the hypothesis that the NB is better intercalated into the longer chain SAMs, leading to a larger number of untethered NB initially contributing to the DPV current in these samples. While we also cannot rule out differences in charge consumption due to rearrangement of the molecules and monolayers upon potential cycling, the trends in the charge ratios between the amine and phenoxazine reactions are consistent with NB intercalation and rejection and clearly follow the linker length dependence we have previously observed.

Alternate to molecular orientation, we also considered the possibility of the amine redox reaction as the cause of the spectral divot for the 588 cm^{-1} SERS mode. To rule out the amine

reaction, we fit each peak to a Lorentzian function and evaluated the spectral characteristics (Fig. S4†). Neither the peak frequency nor width change at potentials positive of the formal potential of the phenoxazine redox reaction ($E^{\circ} \approx -0.25$ V), indicating that reduction and oxidation events at the amine do not perturb the spectral response of the 588 cm^{-1} mode. Moreover, the intensity divot begins before the onset of the amine electrochemical oxidation reaction ($E \approx -0.15$ V) and continues to drop as the potential is swept past the amine reaction.

As a final note on this mechanism: we have drawn the sketches in Fig. 6 to show the most dramatic possible conformations for the tethered NB molecules in SAMs of varying length, but these cartoons do not fully capture the distribution of orientations available to the molecules within the SAM (for example, all oxidized NB molecules are not positioned precisely vertically relative to the substrate, but do show preferential alignment in that direction). As we described in the introduction, AuIFs are highly heterogeneous and there may be defects/local disorder on the surface which allow for a distribution of NB distances and orientations. Nonetheless, because we are performing an ensemble measurement, we are largely averaging out over these effects and see general distant-dependent trends that we have verified over multiple samples. Thus, we are confident that this mechanism provides strong evidence for molecular interactions with SAMs on the electrode surfaces, leading to the unexpected SERS spectroelectrochemical behavior of the NB.

Conclusions

We have evaluated the impact that a tether length has on the SERS spectroelectrochemical response of NB immobilized on Au electrodes. In addition to a change in the electrode–molecule distance, we found that molecular orientation changes with tether length resulting in unique electrochemical and SERS properties. A SERS image derivative analysis and DPV were used to identify the relative molecular orientations for each linker length. We proposed that tethers with lengths shorter than the length of NB molecule show a relatively stable intensity of the 588 cm^{-1} spectral Raman mode at oxidizing potentials due to the rigidity of the short linkage. However, this spectral mode shows an intensity divot when the tether length is greater than or equal to the molecule length, which is explained by the intercalation of the NB redox dye into the hydrophobic SAM layer at oxidizing potentials, which misaligns the transition dipole orientation with the excitation polarization, causing a decrease in intensity. The electrode polarity and solvatochromism were also hypothesized to contribute to the intensity divot. These results demonstrate that in addition to electrode–molecule separation, molecular orientation plays a critical role in the spectroelectrochemical response of Nile Blue tethered to Au electrodes.

Acknowledgements

Work was supported by an AFOSR MURI Award #FA9550-14-1-1003.

References

1 E. C. Le Ru and P. G. Etchegoin, *Annu. Rev. Phys. Chem.*, 2012, **63**, 65–87.
2 Z.-Q. Tian and B. Ren, *Annu. Rev. Phys. Chem.*, 2004, **55**, 197–229.
3 D.-Y. Wu, J.-F. Li, B. Ren and Z.-Q. Tian, *Chem. Soc. Rev.*, 2008, **37**, 1025–1041.
4 E. Cortés, P. G. Etchegoin, E. C. Le Ru, A. Fainstein, M. E. Vela and R. C. Salvarezza, *J. Am. Chem. Soc.*, 2010, **132**, 18034–18037.
5 E. Cortés, P. G. Etchegoin, E. C. Le Ru, A. Fainstein, M. E. Vela and R. C. Salvarezza, *Anal. Chem.*, 2010, **82**, 6919–6925.
6 E. Cortés, P. G. Etchegoin, E. C. Le Ru, A. Fainstein, M. E. Vela and R. C. Salvarezza, *J. Am. Chem. Soc.*, 2013, **135**, 2809–2815.
7 A. J. Wilson and K. A. Willets, *Nano Lett.*, 2014, **14**, 939–945.
8 M. L. Weber, A. J. Wilson and K. A. Willets, *J. Phys. Chem. C*, 2015, **119**, 18591–18601.
9 C. Zong, C.-J. Chen, M. Zhang, D.-Y. Wu and B. Ren, *J. Am. Chem. Soc.*, 2015, **137**, 11768–11774.
10 D. Kurouski, M. Mattei and R. P. Van Duyne, *Nano Lett.*, 2015, **15**, 7956–7962.
11 H.-H. Liu, J.-L. Lu, M. Zhang and D.-W. Pang, *Anal. Sci.*, 2002, **18**, 1339–1344.
12 C. G. Pheeney and J. K. Barton, *Langmuir*, 2012, **28**, 7063–7070.
13 A. J. Wilson, N. Y. Molina and K. A. Willets, *J. Phys. Chem. C*, 2016, DOI: 10.1021/acs.jpcc.6b03962.
14 F. Ni, H. Feng, L. Gorton and T. M. Cotton, *Langmuir*, 1990, **6**, 66–73.
15 I. Doron-Mor, Z. Barkay, N. Filip-Granit, A. Vaskevich and I. Rubinstein, *Chem. Mater.*, 2004, **16**, 3476–3483.
16 B. J. Kennedy, S. Spaeth, M. Dickey and K. T. Carron, *J. Phys. Chem. B*, 1999, **103**, 3640–3646.
17 J. A. Dieringer, A. D. McFarland, N. C. Shah, D. A. Stuart, A. V. Whitney, C. R. Yonzon, M. A. Young, X. Zhang and R. P. Van Duyne, *Faraday Discuss.*, 2006, **132**, 9–26.
18 L.-H. Guo, J. S. Facci and G. McLendon, *J. Phys. Chem.*, 1995, **99**, 8458–8461.
19 H. O. Finklea and D. D. Hanshew, *J. Am. Chem. Soc.*, 1992, **114**, 3173–3181.
20 V. Anandan, R. Gangadharan and G. Zhang, *Sensors*, 2009, **9**, 1295–1305.
21 S. K. Miller, A. Baiker, M. Meier and A. Wokaun, *J. Chem. Soc., Faraday Trans. 1*, 1984, **80**, 1305–1312.
22 E. Bakker, M. Lerchi, T. Rosatzin, B. Rusterholz and W. Simon, *Anal. Chim. Acta*, 1993, **278**, 211–225.

23 J. Stockert, M. Abasolo, A. Blázquez-Castro, R. Horobin, M. Revilla and D. Lombardo, *Biotech. Histochem.*, 2010, **85**, 277–283.
24 D. P. dos Santos, G. F. S. Andrade, M. L. A. Temperini and A. G. Brolo, *J. Phys. Chem. C*, 2009, **113**, 17737–17744.
25 J. Jose, Y. Ueno and K. Burgess, *Chem. – Eur. J.*, 2009, **15**, 418–423.
26 A. Ghanadzadeh Gilani, S. E. Hosseini, M. Moghadam and E. Alizadeh, *Spectrochim. Acta, Part A*, 2012, **89**, 231–237.
27 A. Reigue, B. Auguié, P. G. Etchegoin and E. C. Le Ru, *J. Raman Spectrosc.*, 2013, **44**, 573–581.